coefficient of friction; stability of motion; numerical simulation

Mirosław DUSZA
Warsaw University of Technology, Faculty of Transport
Koszykowa 75, 00-662 Warsaw, Poland
Corresponding author. E-mail: mdusza@wt.pw.edu.pl

THE WHEEL-RAIL CONTACT FRICTION INFLUENCE ON HIGH SPEED VEHICLE MODEL STABILITY

Summary. Right estimating of the coefficient of friction between the wheel and rail is essential in modelling rail vehicle dynamics. Constant value of coefficient of friction is the typical assumption in theoretical studies. But it is obvious that in real circumstances a few factors may have significant influence on the rails surface condition and this way on the coefficient of friction value. For example the weather condition, the railway location etc. Influence of the coefficient of friction changes on high speed rail vehicle model dynamics is presented in this paper. Four axle rail vehicle model were built. The FASTSIM code is employed for calculation of the tangential contact forces between wheel and rail. One coefficient of friction value is adopted in the particular simulation process. To check the vehicle model properties under the influence of wheel-rail coefficient of friction changes, twenty four series of simulations were performed. For three curved tracks of radii R = 3000m, 6000m and ∞ (straight track), the coefficient of friction was changed from 0.1 to 0.8. The results are presented in form of bifurcation diagrams.

WPŁYW WSPÓŁCZYNNIKA TARCIA KOŁA-SZYNY NA STATECZNOŚĆ RUCHU MODELU POJAZDU SZYNOWEGO DUŻYCH PRĘDKOŚCI

Streszczenie. Poprawne oszacowanie współczynnika tarcia w kontakcie kół z szynami jest kluczowym problemem w modelowaniu dynamiki pojazdu szynowego. W badaniach teoretycznych najczęściej przyjmuje się stałą wartość współczynnika tarcia. Jest rzeczą oczywistą, że w warunkach rzeczywistych kilka czynników może mieć znaczący wpływ na stan powierzchni tocznej szyn, a tym samym na wartość współczynnika tarcia, na przykład warunki pogodowe, położenie trasy kolejowej itp. W artykule przedstawiono wyniki badań wpływu zmian współczynnika tarcia na dynamikę modelu pojazdu szynowego. Utworzono model pojazdu czteroosiowego przeznaczonego do ruchu z dużymi prędkościami. Siły w kontakcie koła-szyny są obliczane przy użyciu procedury FASTSIM. Procedura ta przyjmuje jedną stałą wartość współczynnika tarcia w pojedynczej symulacji ruchu. Aby określić wpływ zmian wartości współczynnika tarcia na własności modelu, wykonano dwadzieścia cztery serie symulacji. Na trasach o trzech wartościach promienia łuku R = 3000 m, 6000 m i ∞ (tor prosty) współczynnik tarcia zmieniano od 0,1 do 0,8. Wyniki przedstawiono w postaci wykresów bifurkacyjnych.

1. INTRODUCTION

The area of steel wheel and rail contact is just about 1cm^2. In the tiny contact zone the contact forces that carry the load and roll of the train are transmitted. The contact is absolutely critical to the safe and efficient operation of a railway network. The dynamic behaviour and stability of railway vehicle strongly depend on the wheel-rail interaction [12]. A lot of the complexity of the wheel-rail contact is brought about by the open nature of the system and the constantly varying environmental conditions in terms of, for instance, temperature, humidity and natural contaminants. The phenomenon which occur in the contact area are the subject of researches for a long time. Theoretical works cover wide scope of issues usually directed on:

- Optimisation of the wheel and rail profiles;
- wheel and rail profiles wear limiting;
- limitation to minimum the probability of fatigue cracks appearance;
- creation new models and a fast solution methods to calculate the contact forces.

A broad interdisciplinary approach is needed to create theoretical description of the contact problems. Accuracy of the description and its verification through comparison to experimental results is limited due to complicated measurement process of real system. A few theories of rolling contact are implemented in numerical algorithms and apply to vehicle system dynamics (VSD) packages. The most frequently used are: Kalker's linear theory, Vermeulen-Johnson and Shen-Hedrick-Elkins approaches, FASTSIM algorithm, the Polach method, USETAB program [8, 11]. For the sake of time of calculation all of the VSD packages have to rely on approximations of one or another sort. The CONTACT program is regarded as a complete theory for concentrated contact [4, 10, 11]. However this program is too slow for use in VSD packages in which millions of contact problems must be solved.

To obtain results presented in this paper, tested for many years and used widely FASTSIM algorithm is applied [5, 7]. It based on the so-called simplified theory, where the material constitutive behaviour is approximated. This algorithm is an optional tool available in VI-Rail package used to carry out the researches. The steel wheel rolling on steel rail is a classical example of rolling friction system. But it is known that clear form of rolling friction exists very seldom. Elastic deformations of the wheel and rail contact surface appear under the contact forces effect (Fig. 1). The outside slip appears on the surface of contact zone and inside slip in the wheel and rail deformed layer of material. The wheel and rail materials properties in real circumstances may significantly differ from these for clean state (in the laboratory conditions). The coefficient of friction (μ) is one of the key parameters characterising the wheel – rail contact properties in theoretical researches. The mentioned numerical algorithms intended to calculate the contact, accept one value of coefficient of friction usually. But experiments point to significant range of possible changes of μ in real objects [6]. The minimum value of μ may achieve about 0.1. Such small values are observed on the railway lines located in the deciduous forest. The leaves pick up and take of as an effect of moving train air turbulence, may occur between wheels and rails. The leaves fastened to rails by the pressure adsorb the atmospheric humidity. Additionally iron oxides appear due to the moisture on rail surface. The damped leaves together with the iron oxides constitute some kind of third body layer, which separate the bulk materials in the wheel – rail contact. This way coefficient of friction is significantly reduced. Another reason of μ reduction is the inside surfaces of hi-rail head lubrication in curved track of small radii. The lubricant application make easier the curved track negotiation. Some volumes of the lubricant migrate onto railhead during the vehicles motion. This is undesirable but unavoidable effect. Maximum coefficient of friction value (about 1.0) appears for dry

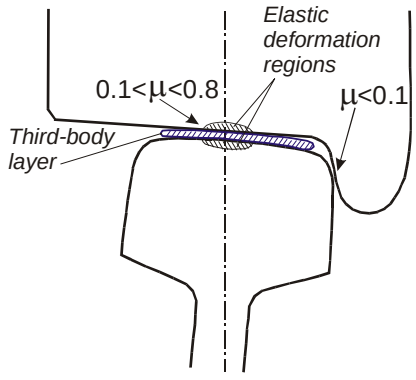

Fig. 1. The wheel-rail contact region
Rys. 1. Obszar kontaktu koło-szyna

railhead and wheel tread surfaces and sand delivery between the surfaces. Almost all weather conditions have influence on μ value. Inappropriate assumption of μ can lead to an underestimation or overestimation of μ. Overestimation of the μ in modelling rail vehicle dynamics may lead to unexpectedly long braking distances, low locomotive traction, and high fuel (energy) consumption [3]. Conversely, when μ is underestimated, unexpected increases in wheel-rail wear and wheel-rail noise may appear during real object operation. Thus, accurate estimation of μ plays a very important role in modelling rail vehicle dynamics, reducing operational and maintenance costs, and increasing safety in the long term, as equipment performance is better anticipated.

This paper represents new results obtained by the author by means of numerical simulations. The influence wheel-rail coefficient of friction variation on rail vehicle model stability is presented. Well known bifurcation approach to stability analysis was applied [4, 9, 10]. Essence of the method consists in creating and then analysis of bifurcation plots. Such plots enable to determine chosen parameters changes in so-called active parameter domain [1, 2, 9, 13-15]. Leading wheelset's lateral displacements y_p (of the 4-axle vehicle) is the chosen, observed and recorded parameter. It represents either stable or unstable solutions in the vehicle velocity (bifurcation parameter) domain. Some rail vehicle – track system parameters (e.g. the suspension parameter values, track gauge, rails inclination, profiles of wheels and rails wear and others) influence on rail vehicle model stability were tested [1, 2, 13-15]. Now the researches focus on the wheel-rail coefficient of friction value. The VI-Rail engineering software codes utilize the FASTSIM numerical procedure [5] to calculate wheel-rail contact forces. The singular value of μ is adopted by the procedure to carry out one simulation process. So to check wide range of μ values influence on rail vehicle stability, 24 series of simulations were executed. For μ increased from 0.1 to 0.8 with the step of changes 0.1, series of simulations in curved tracks of radii R = 3000, 6000m and ∞ (straight track) have been done. Each series consist of a few dozen simulations executed for constant velocity value. The initial velocity value applied was 10m/s usually. Stable stationary solutions exist for such velocity value. In the next simulation process velocity was increased. The last velocity value is the maximum one for which stable solutions (stationary or periodic one) exist. Critical velocity value v_n and character of solutions in the range of velocity under and above the critical value are determined in each series of simulations. The first wheelset lateral displacements y_p are observed. The maximum of leading wheelset lateral displacement absolute value ($|y_p|$max) and peak-to-peak value of y_p (p-t-p y_p) are determined. Couples of bifurcation diagrams that present both these parameters in vehicle velocity domain were accepted as a form of the results presentation (fig. 5…7).

2. THE MODEL

The MBS was build up with the engineering software VI-Rail (ADAMS/Rail formerly). This is the environment, which enables users to create any rail vehicle – track model by assembling typical parts (wheelsets, axleboxes, frames, springs, dampers and any other) and putting typical constrains on each of kinematical pairs. Exemption of users from deriving the equations of motion by themselves is the main advantage of this software. This and many other advantages of the software reduce the time devoted to build the model significantly. The simulation model being tested in the paper consists of vehicle and track. Complete system has 82 kinematic degrees of freedom.

2.1. The vehicle model

Typical 4-axle passenger vehicle model is employed in the simulations (Fig. 2). Vehicle model corresponds to the 127A passenger car of Polish rolling stock. Bogies of the vehicle have 25AN designation in Polish terminology. The model consists of fifteen rigid bodies representing: carbody, two bogies with two solid wheelsets and eight axleboxes. Each wheelset is attached to axleboxes by joint attachment of a revolute type. So rotation of the wheelsets around the lateral axis with respect to axleboxes is only possible. Arm of each axlebox is attached to bogie frame by pin joint (bush type

element). They are laterally, longitudinally and rotary flexible elements. The linear and bi-linear characteristics of the primary and secondary suspension are included in the model. They represent metal (screw) springs and hydraulic dampers of primary and secondary suspension. In addition torsion springs (k_{bcb}) are mounted between car body and bogie frames. To restrict car body – bogie frame lateral displacements, bumpstops with 0.03 m clearance were applied (not visible in Fig. 2). A new S1002 wheel and UIC60 rail pairs of profiles are considered. Non-linear geometry of wheel - rail contact description is assumed. Contact area and other contact parameters are calculated with use of RSGEO subprogram (implemented into VI-Rail). To calculate wheel-rail contact forces, results obtained from RSGEO are utilized. In order to calculate tangential contact forces between wheel and rail, so called non-linear simplified theory of the rolling contact by J.J. Kalker is applied. It is implemented in the computer code FASTSIM [5, 7] used worldwide.

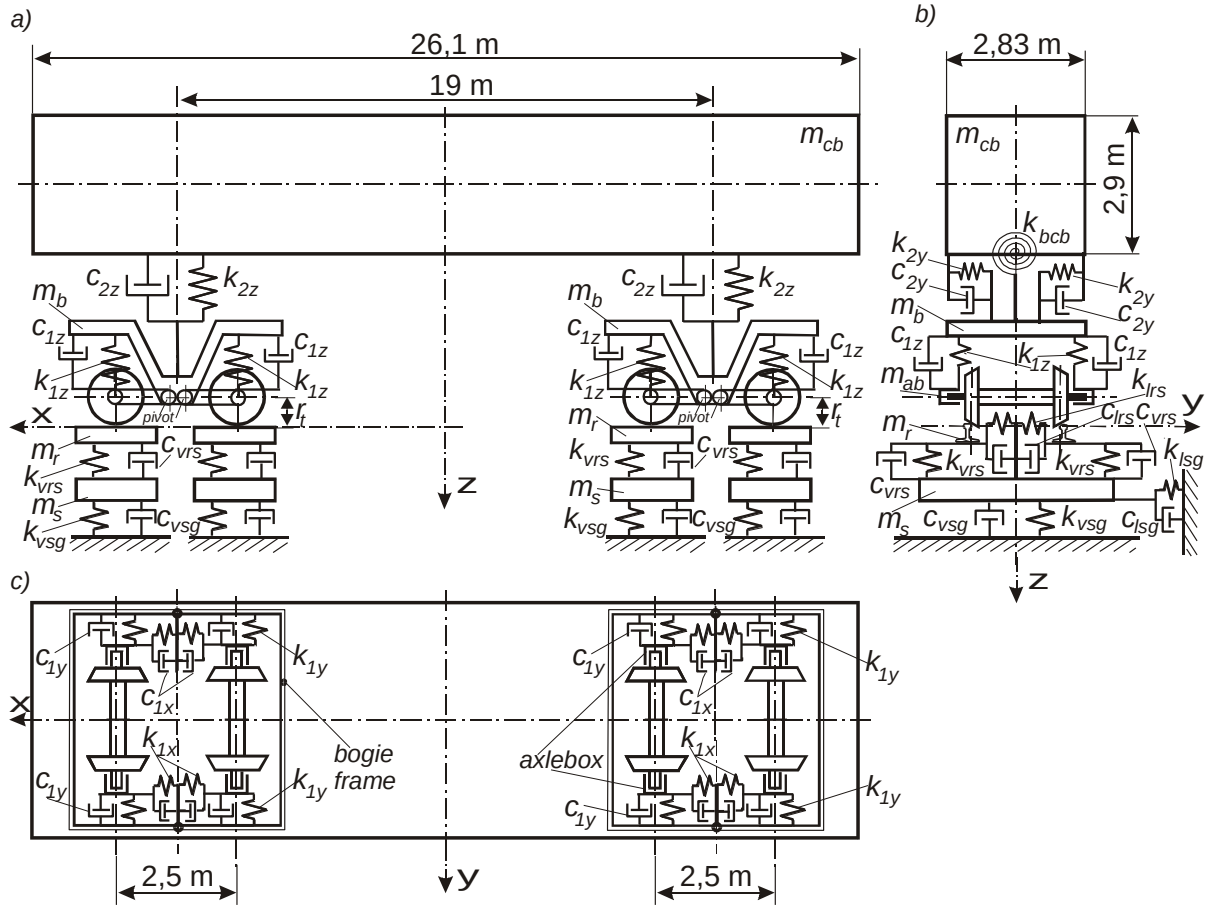

Fig. 2. Vehicle – track nominal model structure: a) side view, b) front view, c) top view
Rys. 2. Struktura modelu nominalnego pojazd – tor: a) widok z boku, b) widok z przodu, c) widok z góry

2.2. Track Model

Discrete, two level, vertically and laterally flexible track models were assumed (Fig. 3). But models of track flexibility are simplified. For low frequency analysis (less than 50 Hz) simplified track model is accepted when dynamics of vehicle motion is considered. Rails and sleepers are treated as a lumped mass (m_r, m_s) of the corresponding rigid bodies. No track irregularities are taken into account. Periodic support of the rails in real track is neglected in the model too. So, the non-inertial type of the moving load is adopted here. Linear elastic springs and dampers connect the track parts (rigid bodies) to each other. Similar approach is used in many works in vehicle dynamics where just low frequency deformations of the track are of the interest, e.g. [3, 4, 8 - 10, 12].

The track has got nominal UIC60 rails with a rail inclination 1:40. Each wheelset is supported by a separate track section consisting of two rail parts and sleepers that correspond to 1m length of typical ballasted real track. Every wheelset – track subsystem has homogenous properties and is independent from one another. Each route of curved track model is composed of short section of straight track, transition curve and regular arc. Constant value of superelevation depending on curve radius value is applied for each curved track route (Table 1).

Table 1

Curve radii tested and track superelevations corresponding to them

Curve radius R [m]	3000	6000	∞
Superelevation h [m]	0.110	0.051	0

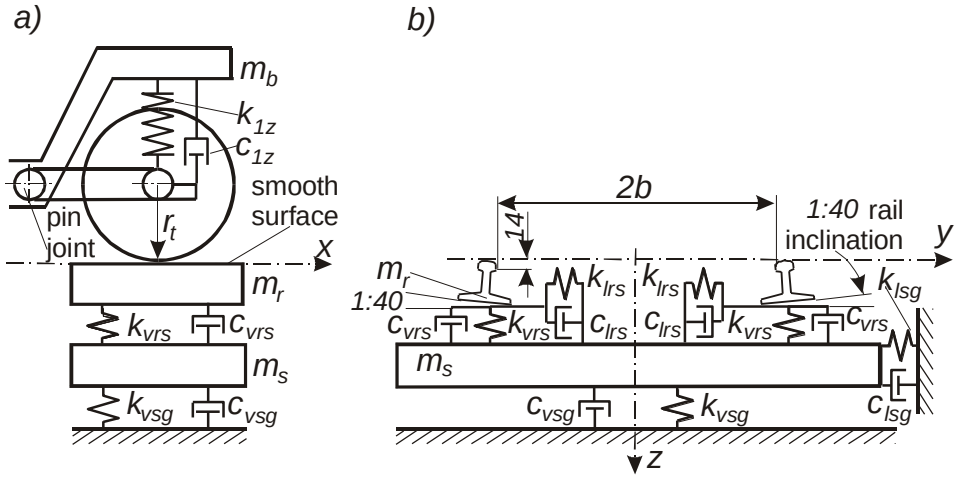

Fig. 3. Track nominal model structure: a) side view, b) cross section view
Rys. 3. Struktura nominalna modelu toru: a) widok z boku, b) w przekroju poprzecznym

Detailed vehicle and track model parameters are collected in Appendix.

3. THE METHOD

Basically, the method used by the author in the present study is based on the bifurcation approach to the analysis of rail vehicle lateral stability. This approach is widely used in the rail vehicle lateral dynamics, e.g. [4, 9, 10, 12 and 1, 2, 13-15]. This method takes account of the stability theory, however is less formal than the theory but more practical instead. In another word, it also makes use of some assumptions and expectations from the system being studied, which are based on the already known general knowledge about the rail vehicle systems. In accordance with that, building the bifurcation plot is the main objective here but formal check if the solutions on this plot are formally stable is not such an objective. That is why one does not adopt some solution as the reference one in this approach and then does not introduce some perturbation into the system to check if the newly obtained solution stays within some narrow vicinity of the reference solution, what definition of the stability (theory) would require. The approach assumes that any solution typical for railway vehicle systems (stationary or periodic) is stable. Such assumption could be accepted based on the understanding within the railway vehicle dynamics that periodic solutions are the self-exciting vibrations that are governed by the tangential forces in wheel-rail contact. Thanks to it, the self-exciting vibrations theory can be used to expect (predict) typical behaviour of the system. Only when

serious doubts about stability appear, formal check for the stability (with the initial conditions variation to introduce the perturbation) is then performed.

On the other hand, another very important reason exists to vary the initial conditions. This is the need to get all the solutions in order to build the complete bifurcation diagram. Varying the initial conditions carefully, widely and knowingly enables to obtain all multiple solutions for the particular velocity v value. It is the case for both the stable and unstable solutions as well as stationary and periodic solutions known in the railway vehicle dynamics. Repeating the procedure for all velocity range makes it possible to get the bifurcation plots, as e.g. Figs. 4a and 4b. As it is seen on these figures the bifurcation plots represent stability properties of the system as they show precisely areas of the stable and unstable solutions, both the stationary and periodic ones. The crucial elements on the plots are saddle-node bifurcation and subcritical Hopf's bifurcation that correspond to the stable solutions lines and velocities v_n and v_c, respectively (see Figs. 4a and 4b). The v_n and v_c are well known in the rail vehicle stability analysis non-linear and linear critical velocities, respectively.

It is worth adding that bifurcation approach, focused on building the bifurcation diagrams, is also suitable to represent less typical behaviours of the railway vehicle systems, as chaotic ones. Then more formal activities are necessary, however.

Interpretation and extension to the above statements, including physical aspects, can be found in [14, 15] where thorough considerations are presented, which enable dipper understanding of the rail vehicle lateral stability analysis. The method presented in [15] is more formal than that in [14].

According with the above the information is given below, referring to the considered objects, on how the bifurcation plots for the needs of the present paper were built. The first part refers to the straight track case, while the second one to the circular curve case.

In the method used, the first bogie's leading wheelset lateral displacements y_p are observed and recorded in time domain (as in Figs. 4c and 4d). The stable stationary solutions can appear (Fig. 4c) in the system. They are typical for vehicle velocity less than the critical value v_n. Sometimes in a curved track for velocity higher than the critical one they appear as well. In case of the stable stationary solutions zero lateral displacements and peak-to-peak values in straight track are observed. In addition, the tested vehicle model is example of hard excitation system, e.g. [14]. It means that some minimum value of initial conditions have to be imposed to initiate periodic solutions (self-exciting vibrations in real system). Alternatively, some other perturbation in the system has to be introduced. Thus, in order to initiate vibrations the straight track test section has got singular lateral irregularity situated 200 m from the track beginning. The irregularity has half of sine function shape. Its amplitude equals 0.006 m and wave length 20 m. So all wheelsets are shifted in lateral direction in straight track during the irregularity negotiation. Afterwards the wheelsets tend to central position (for velocity lower than the critical value v_n) or lateral displacements increase and may change periodically (for velocity equal or bigger then the critical value v_n). The smallest motion velocity for which stable periodic solutions (limit cycles) appear is accepted as a critical value v_n. The step of velocity changes equal 0.1 m/s was applied in particular simulations processes. Hence, the accuracy of critical velocity value determination is equal to 0.1 m/s, too. Existence of periodic solutions (self-exciting vibrations in real object) means also energy dissipation in the system. Two conditions have to be met to initiate the periodic solutions. The first is some minimum value of energy delivered to the system (minimum velocity value in the tested system). The second is application of some minimum value of initial excitation (e.g. track irregularity of sufficient amplitude). The periodic solutions (limit cycles) are generally not desirable in real objects because vibration is always worse than stationary behaviour. On the other hand limited (and constant) value of the amplitude enables safe vehicle motion. Consequently, such type of solutions can be accepted as being the stable one. Amplitude as well as other limit cycle parameters can constitute some indicators of the system state. The maximum of wheelset lateral displacements (y_p max) and their peak-to-peak values (p-t-p y_p) are utilized in the method.

Non-zero lateral displacements (vibrations) appear in the initial part of curved track, usually (as for R = 2000 m in Fig. 4c). It is caused by the lack of balance between lateral (with respect to track plane) forces acting on the vehicle in curve. Another word, the lateral components of centrifugal and gravity forces do not neutralize each other. Stationary value of wheelset lateral displacement becomes

established after enough long time (12 seconds in Fig. 4c). So, stable stationary non-zero solutions exist in curved track for velocity lower than v_n, usually. Exceeding the critical velocity value v_n means self-exciting vibrations appearance. It causes for vehicle model transfer (bifurcation) of solutions from the stable stationary to the stable periodic ones (Fig. 4d). The wheelsets move periodically along lateral axis *y* and rotate round their vertical axis *z*. It is the form of energy dissipation, typical in wheelset-track system. Similarly to the straight track case, two conditions should be fulfilled to initiate the self-exciting vibrations in circular curve too. The first one is some minimum velocity value of wheelset (vehicle). The second one is sufficiently big initial excitation of the wheelset. For the analysis of stability in curved track sections it is not sure if the initial excitation at the beginning of straight track section can play its role sufficiently. On the other hand transition curve negotiation appeared to be quite enough excitation to initiate periodic solutions in the regular curve (if vehicle velocity is equal or exceeds the critical value v_n). That is why the lateral irregularity in straight track is not applied in curved track cases.

In practice, to obtain the results for curved track, compound routes had to be applied. It is the consequence of VI-Rail software feature. It cannot start calculations in a curved track directly. Therefore simulations, which finish in a curved track, have to begin in straight track section (first 3 seconds in Fig. 4c and 4d). Then they pass through transition curve and finally the regular curved track section (R = const.) begins. If the wheelset's lateral motion takes form of limit cycle and exists until end of the test time (15 s usually), the state represents and is called the stable periodic solution (Fig. 4d).

Constant value of velocity is taken in each simulation. Two parameters – maximum of leading wheelset lateral displacement absolute value ($|y_p|$max) and peak-to-peak value of y_p (p-t-p y_p) are determined. Diagrams of these parameters in velocity domain (Fig. 4a and 4b) are created. Both graphs include the lines matching circular track sections of radii from R = 1200 m to $R = \infty$ (straight track). So a few lines are presented in the complete diagrams usually. Each line is created following a series of single simulations for different *v* and the same route. The range of *v* starts at low velocities, passes critical value v_n and terminates in velocities v_d, called sometimes the derailment velocity. The value v_d does not mean the real derailment, however. This is the lowest value of velocity for which results of simulations take no limit cycle shape and no quasi-static shape either. But the vehicle motion is possible often. In addition, if wheelset lateral displacements take large values the climb of wheels on rail head could happen. In curved track, outer wheel may be lift up and can loss contact at velocity v_d sometimes. It is effect of centrifugal force acting and it is treated as a derailment too. The pairs of diagrams like those visible in Figure 4a and 4b, which include results for all tested curve radii, are called a „stability maps" and selected as a form of results presentation.

The meaning of stable motion of vehicle in the current research should be expressed here, now. Just stable stationary solutions (constant value of wheelset lateral displacement y_p) or stable periodic solutions (limit cycle of y_p) are assumed to describe stable vehicle motion. Any other solutions are assumed to be the unstable ones. The periodic motion of wheelset corresponding to its limit cycle is not desirable in real vehicle exploitation of course. On the other hand, limit cycle in the stability analysis means constant peak-to-peak value and frequency of the wheelset lateral displacements. Consequently, if the maximum of wheelset lateral displacement value does not exceed the permissible value, vehicle motion is possible and to some extent safe.

Great practical significance has the non-linear critical velocity v_n. It is a good idea to take it at least a bit higher than velocity permissible for real object (maximum service speed of the vehicle). Stable solutions exist in range of velocity smaller and bigger than the critical value v_n. But distance between the critical value v_n and the derailment value v_d can be significantly different in individual tests. This distance depends on the vehicle – track system parameters (see results). From the practical point of view the critical velocity should be high and distance between critical velocity and derailment velocity possibly long.

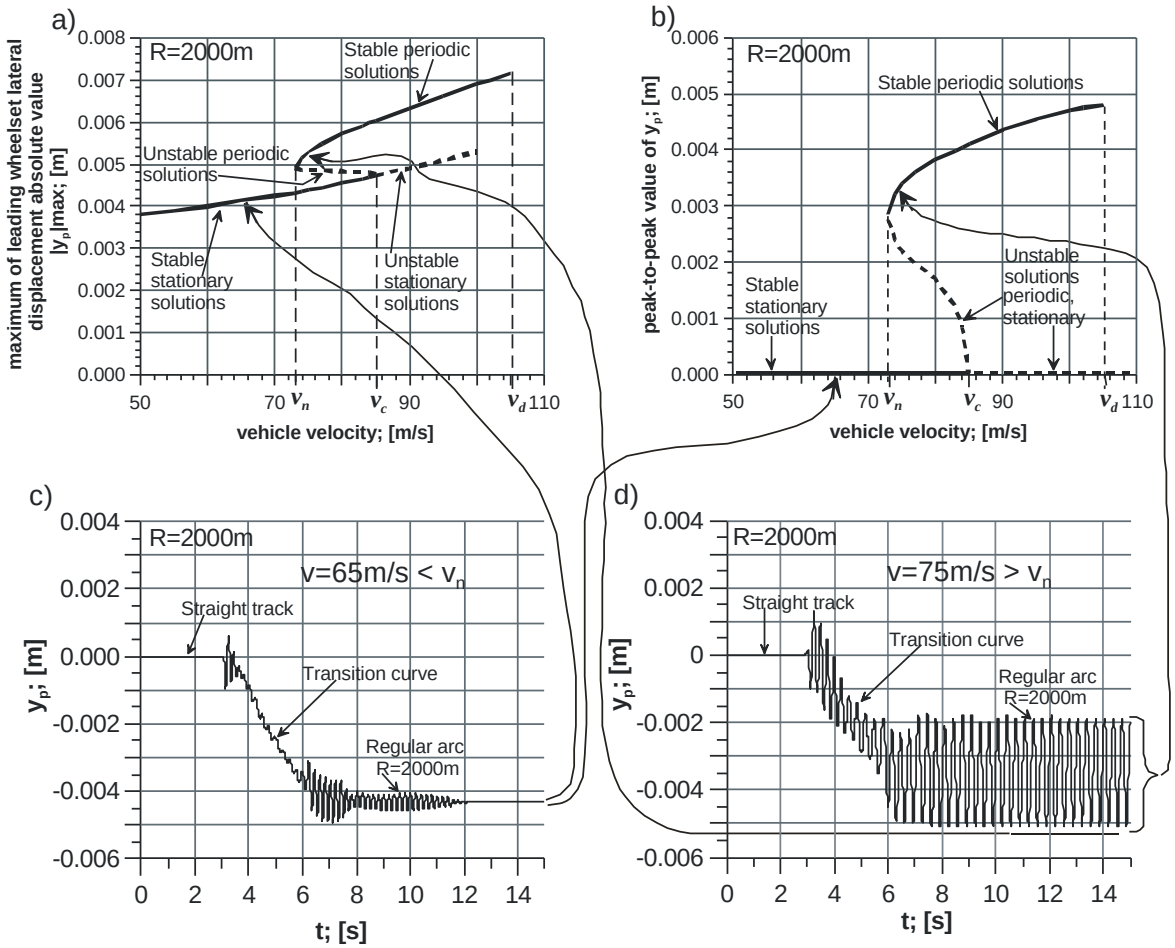

Fig. 4. Scheme of creating the pair of bifurcation plots useful in the curved track analysis
Rys. 4. Schemat metody tworzenia par wykresów bifurkacyjnych w badaniach ruchu po łuku

4. THE RESULTS

Considering the coefficient of friction (μ) influence on rail vehicle model stability, straight track motion was analysed at the beginning. The results are presented in Figure 5. Constant velocity value is applied in each simulation. Just stable stationary solutions exist for velocities lower than 40m/s ($y_p = 0$ and *p-t-p* $y_p = 0$). So, the results for velocity bigger than 40m/s are presented. For eight values of μ increased from 0.1 to 0.8 (with the step 0.1), series of simulations were executed. The velocity of motion is increased in the next simulation (executed for particular μ value) with the step 2m/s. But in case of sudden change of solution value or of solution character the velocity step was dropped to 0.1m/s.

The smallest critical velocity value v_n = 58m/s appears for μ = 0.1. The smallest $|y_p|$max and *p-t-p* y_p exist in this case in comparison to results for bigger μ values. The $|y_p|$max achieves about 0.0067m and *p-t-p* y_p about 0.0134m. Both these parameters increase at the beginning and over the range of critical velocities and then stabilize. Although no derailment indicatives appear the simulations were discontinued at 200m/s. Velocities bigger than 200m/s (720km/h) are too unrealistic to apply in real systems yet. Critical velocity increases to 62m/s for μ = 0.2. Both the observed parameters increase in the initial range and over critical velocities and then stabilize. But values of these parameters are bigger at the same velocity in comparison with the previous case. The series of simulations was stopped at 200m/s in this case too. Next μ was increased to 0.3. The critical velocity value appears at 63.3m/s. It was the biggest critical velocity value in the straight track case. Gentle increase of $|y_p|$max and *p-t-p* y_p is observed in the initial range over the critical velocity values. Then both parameters

increase significantly in the velocity range 100 … 140m/s and stabilize for velocity bigger than 160m/s. Simulations were stopped at 200m/s in this case too. The critical velocity value v_n = 61.8m/s appears for μ = 0.4. Both observed parameters increase in the initial range over the critical velocity values and stabilize for velocities bigger than 100m/s. 129m/s is the maximum velocity value for which stable solutions exist. The $|y_p|$max achieve about 0.0095m and *p-t-p* y_p about 0.0190m at this velocity. Thus significant cut of the velocity range of stable solutions can be observed.

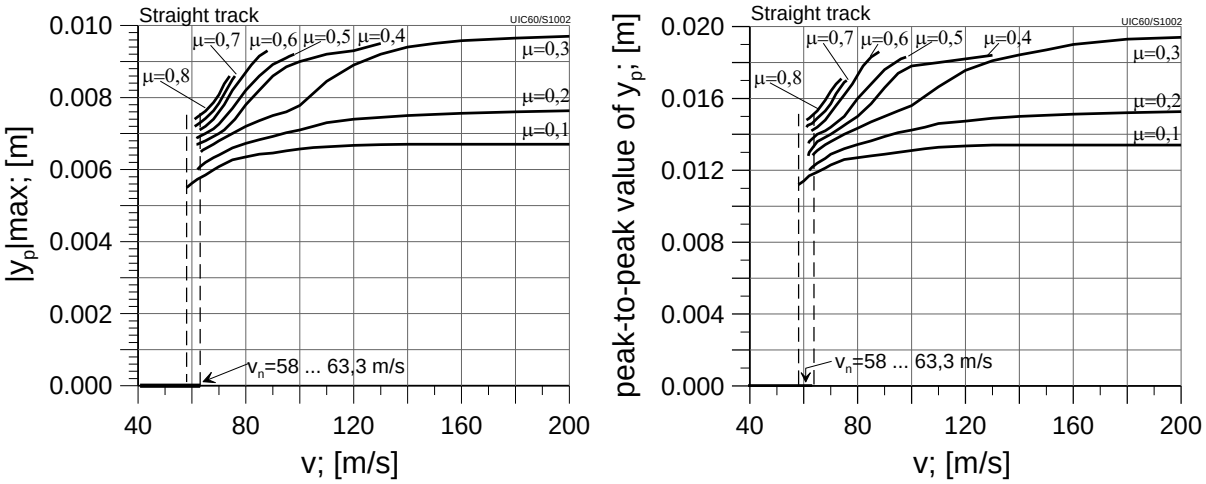

Fig. 5. Maximum of absolute value of leading wheelset lateral displacements ($|y_p|$max) and peak-to-peak value of the leading wheelset lateral displacements versus velocity of motion along straight track for wheel-rail coefficients of friction from 0.1 to 0.8

Rys. 5. Wartości maksymalne z bezwzględnych wartości przemieszczeń poprzecznych pierwszego zestawu kołowego ($|y_p|$max) oraz wartości międzyszczytowe tych przemieszczeń (*peak-to-peak value of* y_p) w funkcji prędkości ruchu na torze prostym dla współczynników tarcia koła – szyny od 0,1 do 0,8

The same critical velocity value 61.8m/s appears for μ = 0.5. The maximum velocity of stable solutions existence is equal 98m/s. Critical velocity slightly increase to 62.8m/s for μ = 0.6. But the maximum velocity of stable solutions decreases to 89m/s. $|y_p|$max = 0.0094m and *p-t-p* y_p = 0.0188m at this velocity. Critical velocity value v_n = 61m/s for the biggest μ values 0.7 and 0.8. Maximum velocity values for which stable solutions exist are equal 78m/s and 75m/s for μ = 0.7 and 0.8, respectively. Thus the ranges over the critical velocity of stable solutions are short in comparison to these for smaller μ values.

Similar range of simulations for curved track motion was executed. Big curve radius R = 6000m was applied at the beginning. The results are presented in Fig. 6. Stable stationary solutions exist for velocity smaller than 40m/s (similarly to straight track case). It means that *p-t-p* y_p = 0 but $y_p \neq 0$. It is an effect of balance lack between lateral forces acting on vehicle while curve track negotiating. Wheelset lateral displacements decrease from about 0.0015m to 0.0012m in velocity range 40 …62m/s. The smallest critical velocity value 62m/s appear for μ = 0.1. The y_p increases to 0.0057m in the initial range over the critical velocity and then decreases to about 0.001m at velocity 95m/s. Bifurcation of solutions appears at this velocity value. Stable periodic solutions disappear, *p-t-p* y_p = 0 and $|y_p|$max rises from 0.001m to 0.0043m. Stable stationary solutions exist for velocities bigger than 95m/s. Increase of $|y_p|$max to 0.0061m can be observed and 140m/s is the maximum velocity value for which stable solution exists. The critical velocity increased to 66.7m/s for bigger μ = 0.2. Increase of *p-t-p* y_p and $|y_p|$max for analogous velocities in comparison to previous case (for μ = 0.1) can be observed. Both observed parameters increase in the range of velocity from critical value to about 96m/s. Then they decrease and bifurcation point appears at velocity 115m/s. The *p-t-p* y_p drops to zero and $|y_p|$max increases from about 0.001m to 0.002m. Stable stationary solutions exist above velocity 115m/s. The $|y_p|$max increases to about 0.0061m at 142m/s and this is the maximum velocity for which

stable solution exists. Coefficient of friction μ = 0.3 was applied next. The critical velocity v_n = 69.5m/s. Both of observed parameters achieve maximum, $|y_p|$max = 0.0075m and *p-t-p* y_p = 0.0144m, at velocity 105m/s. Then they decrease and bifurcation point appears at velocity 126m/s.

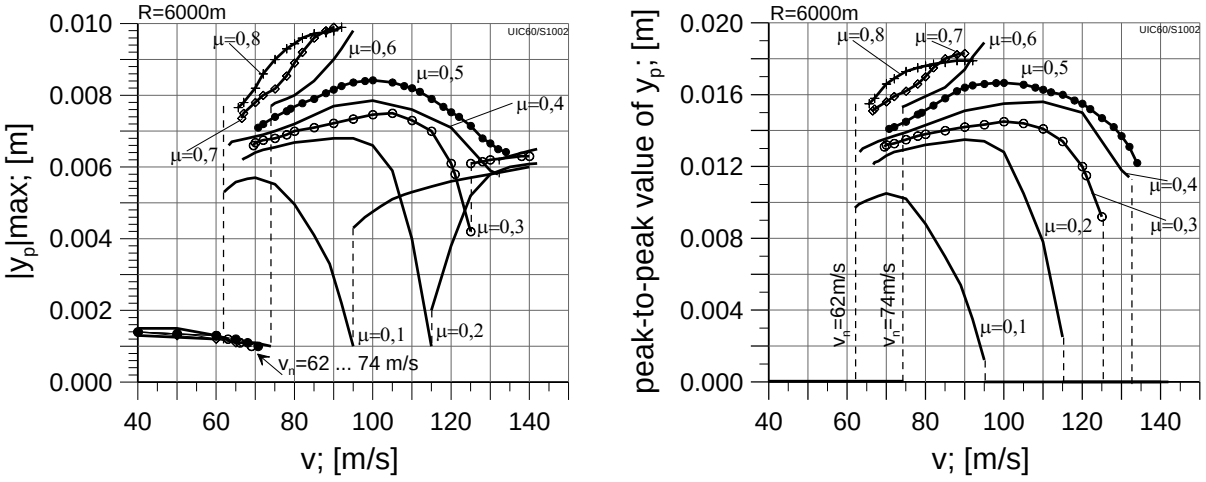

Fig. 6. Maximum of absolute value of leading wheelset lateral displacements ($|y_p|$max) and peak-to-peak value of the leading wheelset lateral displacements versus velocity of motion along curved track of radius R = 6000m for wheel-rail coefficients of friction from 0.1 to 0.8

Rys. 6. Wartości maksymalne z bezwzględnych wartości przemieszczeń poprzecznych pierwszego zestawu kołowego ($|y_p|$max) oraz wartości międzyszczytowe tych przemieszczeń (*peak-to-peak value of* y_p) w funkcji prędkości ruchu na torze o promieniu łuku R = 6000m dla współczynników tarcia koła – szyny od 0,1 do 0,8

Stable stationary solutions exist for velocities up to 140m/s. The critical velocity decreases to 63m/s for μ = 0.4. The observed parameters achieve maximum $|y_p|$max = 0.0078m and *p-t-p* y_p = 0.0157m in the range of velocity 100 … 110m/s. Next they decrease and bifurcation point appears at 133m/s. Stable stationary solutions exist until 142m/s. Increase of critical velocity to 70.7 m/s is observed for μ = 0.5. Maximum of the observed parameters appears in the range of velocity 95 …105m/s, $|y_p|$max = 0.0085m and *p-t-p* y_p = 0.0165m. Stable periodic solutions exist in the range of velocities up to 134m/s. The applied μ = 0.5 is the minimum μ value for which stable periodic solutions exist in whole over critical range of velocity (lack of bifurcation points). Critical velocity value v_n = 74m/s for coefficient of friction μ = 0.6 appears. It is the biggest v_n value among the eight μ cases tested. $|y_p|$max increase from 0.0077m at critical velocity to 0.0098m at 95m/s (the maximum velocity for which stable solutions exists). The *p-t-p* y_p increase from 0.0152m to 0.019m in the same velocity range. So, significant decrease of the velocity range (in comparison with the smallest μ value cases) for which stable solutions exist can be observed. The critical velocities achieve 66.5m/s and 65.6m/s for the biggest μ values tested, 0.7 and 0.8 respectively. Both observed parameters increase and achieve $|y_p|$max = 0.0098m and *p-t-p* y_p = 0.0182m at the maximum velocities for which stable solutions exist, i.e. 90 and 92m/s respectively.

Curved track motion for smaller curve radius R = 3000m was analysed next. The results are presented in Figure 7. The smallest μ value 0.1 was applied at the beginning. Stable stationary solutions exist for velocities up to 55.4m/s. The $|y_p|$max achieves about 0.003m and *p-t-p* y_p = 0 for smaller velocities. At the critical velocity v_n = 55.4m/s periodic solutions appear. Both observed parameters increase to $|y_p|$max = 0.0047m and *p-t-p* y_p = 0.0058m at velocity about 64m/s. Then both parameters decrease to 0.0016m and 0.001m, respectively and bifurcation point appears at velocity 76m/s. Stable stationary solutions exist up to 112m/s. $|y_p|$max increases from 0.0046m to 0.0061m. The critical velocity increases to 58m/s for μ = 0.2. Maximum of both observed parameters fall at velocity about 74m/s. The $|y_p|$max = 0.0059m and *p-t-p* y_p = 0.0098m. Then both parameters decreases

and bifurcation point appears at velocity 86m/s. Stable stationary solutions exist up to 106m/s. The critical velocity increases to 66.6m/s for μ increased to 0.3. Similarly to previous cases both observed parameters rise in the initial range over the critical velocity values and the maximum is achieved at about 76m/s, $|y_p|$max = 0.0066m and *p-t-p* y_p = 0.0124m.

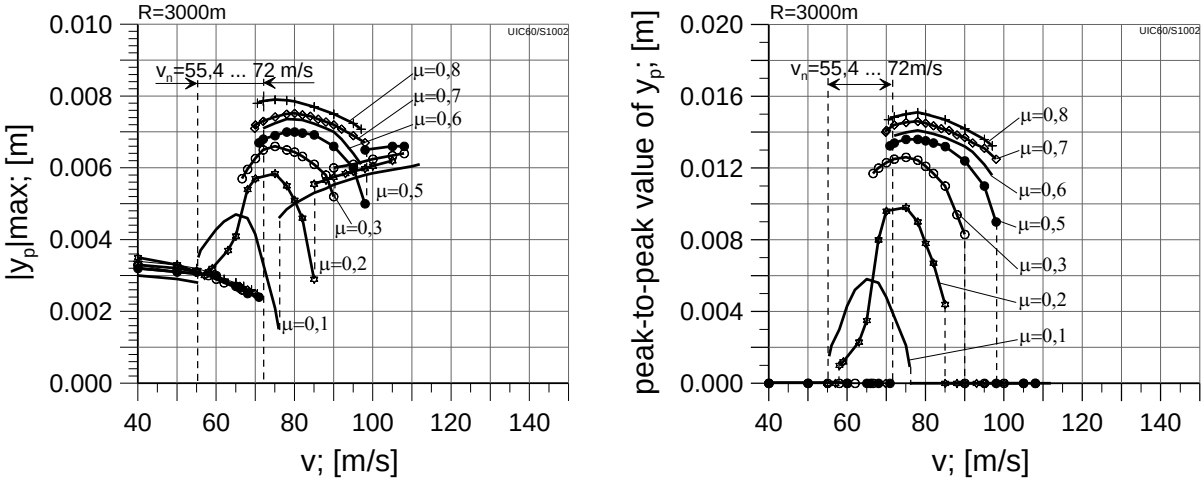

Fig. 7. Maximum of absolute value of leading wheelset lateral displacements ($|y_p|$max) and peak-to-peak value of the leading wheelset lateral displacements versus velocity of motion along curved track of radius R = 3000m for wheel-rail coefficients of friction from 0.1 to 0.8

Rys. 7. Wartości maksymalne z bezwzględnych wartości przemieszczeń poprzecznych pierwszego zestawu kołowego ($|y_p|$max) oraz wartości międzyszczytowe tych przemieszczeń (*peak-to-peak value of* y_p) w funkcji prędkości ruchu na torze o promieniu łuku R = 3000m dla współczynników tarcia koła – szyny od 0,1 do 0,8

Then both parameters decrease and bifurcation of solutions appears at 90m/s. Stable stationary solutions exist for velocity rising up to 108m/s. Critical velocity value increases to 70.9m/s for μ = 0.5. The solution slightly increases at the beginning range over the critical velocities. Then it decreases and bifurcation point appears at velocity 98m/s. Stable stationary solutions exist for velocities up to 108m/s. The biggest critical velocity value 72m/s appears for μ = 0.6. Periodic solutions exist up to 96m/s. No bifurcation points are observed for this and bigger μ values in the range over the critical velocity. The critical velocity values achieve 69.8 and 70.5m/s for the biggest μ values, 0.7 and 0.8 respectively. Stable periodic solutions exist up to 98 and 96m/s in these cases. Both observed parameters achieve maximum values here in comparison to the smallest μ values cases.

5. CONCLUSIONS

Significant influence of wheel-rail coefficient of friction μ on rail vehicle stability can be observed. Increase of μ from 0.3 to 0.5 means significant decrease of the range of velocities for which stable solutions exists in the case of straight track motion. From theoretical point of view, stable motion at velocity of 100m/s with μ = 0.3 is possible. Increase of μ to 0.5 (or more) makes the motion unstable (derailment of vehicle). Increase of wheelset lateral displacements y_p according to μ increase can be observed too. It is not desirable effect also. But the μ influence on critical velocity value is slight (in the range of 5.3m/s). Some different features in curved track can be observed. The range of v_n changes for different μ values achieves 12m/s for R = 6000m. The range increases to 16.6m/s for smaller R = 3000m. So increasing μ influence on v_n can be observed while R decreases. No regularity of v_n dependence on μ value can be observed. The v_n achieves minimum for μ = 0.1 and maximum for μ = 0.6 usually. Bifurcation of solutions from stable periodic to stable stationary for velocities bigger than the critical value does not constitute the emergency of derailment in the real system.

References

1. Dusza, M. & Zboiński, K. Bifurcation approach to the stability analysis of rail vehicle models in a curved track. *The Archives of Transport*. 2009. Volume XXI. No. 1-2. P. 147-160.
2. Dusza, M. The study of track gauge influence on lateral stability of 4-axle rail vehicle model. *The Archives of Transport.* 2014. Volume XXX. No. 2. P. 7-20.
3. HyunWook Lee & Corina Sandu Carvel Holton Dynamic model for the wheel-rail contact friction. *Vehicle System Dynamics.* 2012. Vol. 50. No. 2. P. 299-321.
4. Iwnicki, S. (editor). *Handbook of Railway Vehicle Dynamics.* London, New York: Taylor & Francis Group. LLC. 2006.
5. Kalker, J.J. A fast algorithm for the simplified theory of rolling contact. *Vehicle System Dynamics.* 1982. Vol. 11. P. 1-13.
6. Olofsson, U. & Zhu, Y. & Abbasi, S. & Lewis, R. & Lewis, S. Tribology of the wheel-rail contact – aspects of wear, particle emission and adhesion. *Vehicle System Dynamics.* 2013. Vol. 51. No. 7. P. 1091-1120.
7. Piotrowski, J. Kalker's algorithm Fastsim solves tangential contact problems with slip-dependent friction and friction anisotropy. *Vehicle System Dynamics*. 2010. Vol. 48. No 7. P. 869-889.
8. Polach, O. Characteristic parameters of nonlinear wheel/rail contact geometry. *Vehicle System Dynamics.* 2010. Vol. 48. Supplement. P. 19-36.
9. Schupp, G. Computational Bifurcation Analysis of Mechanical Systems with Applications to Rail Vehicles. *Vehicle System Dynamics*. 2004. Vol. 41. Supplement. P. 458-467.
10. Shabana, A.A. & Zaazaa, K.E. & Sugiyama, H. *Railroad Vehicle Dynamics a Computational Approach.* London, New York: Taylor & Francis Group. LLC. 2008.
11. Vollebregt, E.A.H. & Iwnicki, S.D. & Xie G. & Shackleton, P. Assessing the accuracy of different simplified frictional rolling contact algorithms. *Vehicle System Dynamics*. 2012. Vol. 50. No. 1. P. 1-17.
12. Wilson, N. & Wu, H. & Tournay, H. & Urban, C. Effects of wheel/rail contact patterns and vehicle parameters on lateral stability. *Vehicle System Dynamics*. 2010. Vol. 48. Supplement. P. 487-503. In: *21st International Symposium IAVSD.* Stockholm, Sweden. 2009.
13. Zboiński, K. & Dusza, M. Development of the method and analysis for non-linear lateral stability of railway vehicles in a curved track. *Vehicle System Dynamics*. 2006. Vol. 44. Supplement. P. 147-157. In: *Proceedings of 19th IAVSD Symposium.* Milan. 2005.
14. Zboiński, K. & Dusza, M. Self-exciting vibrations and Hopf's bifurcation in non-linear stability analysis of rail vehicles in curved track. *European Journal of Mechanics*. *Part A/Solids*. 2010. Vol. 29. No. 2. P. 190-203.
15. Zboiński, K. & Dusza, M. Extended study of rail vehicle lateral stability in a curved track. *Vehicle System Dynamics.* 2011. Vol. 49. No. 5. P. 789-810.

Appendix

Table A1

Mass parameters

Variable	Description	Unit	Value
m_{cb}	Car body mass	kg	32 000
m_b	Bogie frame mass	kg	2 600
m_w	Wheelset mass	kg	1 800
m_{ab}	Axle box mass	kg	100
m_r	Rail mass	kg	60
m_s	Sleeper mass	kg	500

Table A2

Vehicle model suspension parameters

Variable	Description	Unit	Value	Comment
k_{1x}	Longitudinal primary suspension stiffness	N/m	30 000 000	
k_{1y}	Lateral primary suspension stiffness	N/m	50 000 000	
k_{1z}	Vertical primary suspension stiffness	N/m	732 000	Preload force 46 500 N
c_{1x}	Longitudinal primary suspension damping	N·s/m	0	
c_{1y}	Lateral primary suspension damping	N·s/m	0	
c_{1z}	Vertical primary suspension damping	N·s/m	Linear damping 7 000 Series stiffness 600 000	Nonlinear with series stiffness
k_{2x}	Longitudinal secondary suspension stiffness	N/m	1 600 000	
k_{2y}	Lateral secondary suspension stiffness	N/m	1 600 000	
k_{2z}	Vertical secondary suspension stiffness	N/m	4 300 000	Preload force 80 000 N
c_{2x}	Longitudinal secondary suspension damping	N·s/m	0	
c_{2y}	Lateral secondary suspension damping	N·s/m	Linear damping 1 Series stiffness 6 000 000	Nonlinear with series stiffness
c_{2z}	Vertical secondary suspension damping	N·s/m	Linear damping 20 000 Series stiffness 6 000 000	Nonlinear with series stiffness
k_{bcb}	Bogie frame – car body secondary roll stiffness	N·m/rad	16 406	Torsion spring

Table A3

Track model parameters

Variable	Description	Unit	Value
k_{vrs}	Rail – sleeper vertical stiffness	N/m	50 000 000
k_{lrs}	Rail – sleeper lateral stiffness	N/m	43 000 000
c_{vrs}	Rail – sleeper vertical damping	N·s/m	200 000
c_{lrs}	Rail – sleeper lateral damping	N·s/m	240 000
k_{rrs}	Rail – sleeper rolling stiffness	N/rad	10 000 000
c_{rrs}	Rail – sleeper rolling damping	N·s/rad	10 000
k_{vsg}	Sleeper – ground vertical stiffness	N/m	1 000 000 000
k_{lsg}	Sleeper – ground lateral stiffness	N/m	37 000 000
c_{vsg}	Sleeper – ground vertical damping	N·s/m	1 000 000
c_{lsg}	Sleeper – ground lateral damping	N·s/m	240 000
k_{rsg}	Sleeper – ground rolling stiffness	N·m/rad	10 000 000
c_{rsg}	Sleeper – ground rolling damping	N·m·s/rad	10 000

Table A4

Inertia parameters

Variable	Description	Unit	Value
i_{cbxx}	Car body inertia	kg·m^2	56 800
i_{cbyy}		kg·m^2	1 970 000
i_{cbzz}		kg·m^2	1 970 000
i_{bfxx}	Bogie frame inertia	kg·m^2	1 722
i_{bfyy}		kg·m^2	1 476
i_{bfzz}		kg·m^2	3 067
i_{wxx}	Wheelset inertia	kg·m^2	1 120
i_{wyy}		kg·m^2	112
i_{wzz}		kg·m^2	1 120
i_{axx}	Axlebox inertia	kg·m^2	20
i_{ayy}		kg·m^2	12
i_{azz}		kg·m^2	20

Table A5

Outside dimensions

Variable	Description		Unit	Value
l_{cb}	Car body	length	m	26.1
w_{cb}		width	m	2.83
h_{cb}		height	m	2.9
l_{bf}	Bogie frame	length	m	3.06
w_{bf}		width	m	2.16
h_{bf}		height	m	0.84
$2a$	Wheelset	wheelbase	m	2.5
$2c$		axle length	m	2.0
$2b$		rolling circles distance	m	1.5
r_t		radius	m	0.46

Parameters Arrangement in Simulations:

The VI-Rail software enables users to arrange and adjust many of the computational parameters. The simulation specification, selected method of mathematical description of real elements, and equation solver procedure choice have significant influence on the final results. List of the parameters applied in each simulation is presented below.

- Simulation time – 15 s;
- Number of Steps – 2500;
- Contact Configuration File – mdi_contact_tab.ccf;
- Track Type – flexible;
- Wheel – rail coefficient of friction (variable) – 0.1 … 0.8;
- Young Modulus – 2.1E+11;
- Poisson's Ratio – 0.27;
- Cant Mode – Low Rail;
- Solver Selection – F77;
- Solver Dynamics Setting: Integrator – GSTIFF, Formulation – I3.

Received 23.11.2013; accepted in revised form 19.08.2015